New Phytologist

Limits of thermal and hydrological tolerance in a foundation tree species (*Populus fremontii*) in the desert southwestern United States

Madeline E. Moran[1], Luiza M. T. Aparecido[2], Dan F. Koepke[3], Hillary F. Cooper[4], Christopher E. Doughty[5], Catherine A. Gehring[4], Heather L. Throop[1,2], Thomas G. Whitham[4], Gerard J. Allan[4] and Kevin R. Hultine[3]

[1]School of Life Sciences, Arizona State University, Tempe, AZ 85287, USA; [2]School of Earth and Space Exploration, Arizona State University, Tempe, AZ 85287, USA; [3]Department of Research, Conservation and Collections, Desert Botanical Garden, Phoenix, AZ 85008, USA; [4]Department of Biological Sciences and Center for Adaptable Western Landscapes, Northern Arizona University, Flagstaff, AZ 86011, USA; [5]School of Informatics, Computing, and Cyber Systems, Northern Arizona University, Flagstaff, AZ 86011, USA

Author for correspondence:
Kevin R. Hultine
Email: khultine@dbg.org

Received: *26 May 2023*
Accepted: *5 August 2023*

New Phytologist (2023) **240:** 2298–2311
doi: 10.1111/nph.19247

Key words: chlorophyll *a* fluorescence, groundwater dependent ecosystems, leaf temperature, leaf turgor loss point, local adaptation, *Populus fremontii*, stomatal conductance.

Summary

- *Populus fremontii* is among the most dominant, and ecologically important riparian tree species in the western United States and can thrive in hyper-arid riparian corridors. Yet, *P. fremontii* forests have rapidly declined over the last decade, particularly in places where temperatures sometimes exceed 50°C.
- We evaluated high temperature tolerance of leaf metabolism, leaf thermoregulation, and leaf hydraulic function in eight *P. fremontii* populations spanning a 5.3°C mean annual temperature gradient in a well-watered common garden, and at source locations throughout the lower Colorado River Basin.
- Two major results emerged. First, despite having an exceptionally high T_{crit} (the temperature at which Photosystem II is disrupted) relative to other tree taxa, recent heat waves exceeded T_{crit}, requiring evaporative leaf cooling to maintain leaf-to-air thermal safety margins. Second, in midsummer, genotypes from the warmest locations maintained lower midday leaf temperatures, a higher midday stomatal conductance, and maintained turgor pressure at lower water potentials than genotypes from more temperate locations.
- Taken together, results suggest that under well-watered conditions, *P. fremontii* can regulate leaf temperature below T_{crit} along the warm edge of its distribution. Nevertheless, reduced Colorado River flows threaten to lower water tables below levels needed for evaporative cooling during episodic heat waves.

Introduction

Projected increases in sub-continental-scale mean annual, seasonal, and monthly temperatures due to climate change are well established with relatively strong agreement among global circulation models (Watanabe *et al.*, 2010; Dufresne *et al.*, 2013; Zhao *et al.*, 2021). What is not as well understood is the extent to which future climate change will impact extreme temperature events, such as episodic heat waves (Guirguis *et al.*, 2018; Wobus *et al.*, 2018). Some of the most frequent and intense summer heat waves on the planet are occurring in the subtropical regions of North America, including the desert southwestern United States and northern Mexico, where temperatures are regularly exceeding 45°C (Zscheischler & Seneviratne, 2017; Overpeck & Udall, 2020; Tillman *et al.*, 2020; Fischer *et al.*, 2021). Model simulations indicate that mean summer temperatures in the southwestern United States and northern Mexico will increase from historic means by 1.9°C by 2050 to 5.0°C by the end of the century (Cayan *et al.*, 2013). Although the return interval of episodic heat waves is difficult to predict, model outputs indicate that 100-yr heat wave events in the southwestern United States will occur around threefold more frequently with a global temperature increase of 2.0°C in relation to historic conditions (Russo *et al.*, 2019).

The lower Colorado River corridor that extends from Lake Mead near Boulder City, Nevada, to the river's terminus at the Sea of Cortez in northwestern, Mexico, is among the warmest regions in North America, experiencing temperatures that approach, or even exceed 50°C in midsummer, with more frequent and intense heat waves predicted (Tillman *et al.*, 2020; Bennett *et al.*, 2021). As a consequence of these novel climate conditions, the highly heat adapted riparian flora that persist along the lower Colorado River corridor are at risk of rapidly becoming maladapted to their local environment. Compounding

the impacts of heat stress are river flows that have fallen dramatically below historic levels as a reflection of over-allocation of river water and over two decades of historic drought (Woodhouse *et al.*, 2010; Williams *et al.*, 2020, 2022). Greatly reduced river flows will likely lower water tables that support riparian tree taxa in ways that will further exacerbate the impacts of episodic heat waves (Tillman *et al.*, 2020).

Among the most widely distributed and ecologically important riparian tree species in the southwestern United States and northern Mexico is the iconic Fremont cottonwood (*Populus fremontii* Sarg.). Although *P. fremontii* is highly intolerant of soil water limitations and, thus. its distribution is limited to stream margins and wetland areas, it is by far the most dominant native riparian tree species along the hyper-arid lower Colorado River. This species supports diverse ecosystem services and creates a hotspot of biodiversity in an arid landscape that is of great conservation concern (Ferrier *et al.*, 2012; Bangert *et al.*, 2013). *Populus fremontii* is highly dependent on shallow groundwater availability for survival (Stromberg, 1993; Snyder & Williams, 2000; Rood *et al.*, 2003; Hultine *et al.*, 2010). On the warm edge of its distribution (i.e. along the lower Colorado River), the soil water requirements for *P. fremontii* survival are amplified by the necessity to cool leaves below a critical threshold to maintain photosynthetic gas exchange and leaf longevity over the summer (Hultine *et al.*, 2020b). Thus, the reduction in river discharge into the lower Colorado River could dramatically reduce what is likely already a narrow hydrological niche for *P. fremontii* (Horton *et al.*, 2003; Hultine *et al.*, 2020b; Fig. 1).

Leaf thermal safety can be maintained by either evaporative cooling and/or establishing high thermal tolerance during heat waves. Leaf thermal tolerance is often characterized in relation to electron transport capacity of Photosystem II (PSII): one of the most thermally sensitive components of photosynthesis (Weis & Berry, 1988; Knight & Ackerly, 2003; Geange *et al.*, 2021). One way to evaluate changes in Photosystem II in response to thermal stress is to measure minimum chlorophyll *a* fluorescence (F_o) over different temperature conditions since electron transport capacity of PSII is mechanistically linked to F_o (Maxwell & Johnson, 2000). The temperature response of F_o typically follows a pattern, whereby levels remain relatively constant with moderate heating, before F_o increases sharply at higher temperatures and then declines sharply as temperatures continue to increase (Knight & Ackerly, 2002; O'Sullivan *et al.*, 2013, 2017). Here, we define leaf thermal tolerance thresholds as the critical temperature in which electron transport of PSII is initially disrupted (T_{crit}), when an increase in temperature results in a rapid rise in F_o determined at the point of intersection of two lines, representing the flat and steep parts of the F_o – temperature response curve (Knight & Ackerly, 2002). This inflection point between negligible and rapid increases in F_o likely reflects increased membrane fluidity and the dissociation of membrane-bound proteins involved with electron transport capacity of PSII (Schreiber & Barry, 1977; Hüve *et al.*, 2011). Previous studies indicate that T_{crit} can vary among species, within species, and even within individual plants and is often correlated with previous temperature exposure (Knight & Ackerly, 2002; O'Sullivan *et al.*, 2017; Drake *et al.*, 2018; Perez & Feeley, 2020; Slot *et al.*, 2021) and leaf morphology (Knight & Ackerly, 2003; Slot *et al.*, 2021).

We evaluated high temperature tolerance of leaf metabolism, leaf thermoregulation, and leaf hydraulic function in genotypes from eight *P. fremontii* populations planted in an experimental common garden and at source population field locations across a broad temperature gradient within the lower Colorado River Basin. The common garden was located at the extreme warm

Fig. 1 Photographs of a dead stand of *Populus fremontii* trees along the lower Bill Williams River in west central Arizona, USA, at its confluence with the Colorado River in March 2017, following multiple years of drought and heat stress. Photo credits: Hillary Cooper, Tom Whitham.

edge of *P. fremontii's* distribution, providing a unique opportunity to assess local adaptation to heat stress, thermal tolerance thresholds, and potential physiological trade-offs for coping with extreme heat wave events that are forecasted to increase in frequency and intensity with climate change in the desert southwestern United States. We tested the following inter-related hypotheses: (1) T_{crit} would be positively correlated with mean annual temperature of source population location; (2) minimum daytime stomatal conductance (g_{smin}) in midsummer would be positively correlated with mean annual temperature of source populations; (3) midday T_{leaf} would be negatively correlated with mean annual temperature of source population, reflecting greater evaporative cooling from higher g_{smin} values (i.e. Hypothesis 2); and (4) as a consequence of selection to maintain a higher g_{smin}, drought tolerance – determined by leaf turgor loss point (Ψ_{TLP}) – would be correlated with mean annual temperature of source population.

In addition to testing the four hypotheses above, we compared T_{crit} measured in leaves collected from *P. fremontii* source sites with previously published leaf T_{crit} data from 177 species, spanning a 25 plus °C range in mean maximum temperatures during the warmest month (O'Sullivan *et al.*, 2017). We then related T_{crit} measured in leaves from *P. fremontii* source location to the hottest air temperature recently experienced at each population location. Here, we define leaf thermal safety margin as the difference between T_{crit} and maximum air temperature (T_{smax}) experienced during extreme heat wave events; similar to definitions used by O'Sullivan *et al.* (2017). These comparisons provide context for whether *P. fremontii* genotypes occurring in the warm edge of its distribution are particularly well adapted to heat exposure relative to other tree taxa, and if so, whether warm-adapted genotypes will likely cope with current and forecasted heat exposure along the lower Colorado River.

Materials and Methods

Description of common garden and source populations

Populus fremontii (Wats.) exhibits substantial genetic variation throughout its range (Cushman *et al.*, 2014), which encompasses broad environmental gradients extending from Mexico, Arizona and California in the south, and reaching northward into Nevada and northern Utah (Eckenwalder, 1977). Extensive field collections reveal that *P. fremontii* is strongly differentiated into three distinctive genetic groups, and genetic variation among populations is primarily driven by climate gradients and connectivity along river networks (Cushman *et al.*, 2014; Ikeda *et al.*, 2017; Bothwell *et al.*, 2023). Among these, genetic groups is a distinctive ecotype within the Sonoran Desert region comprising the lower Colorado River Basin (Ikeda *et al.*, 2017).

In 2014, an experimental common garden was established along the lower Colorado River near Yuma, AZ, USA (32.850, −114.493, 49 m, Fig. 2), from replicate cuttings collected from 12 *P. fremontii* genotypes per 16 source populations representing two of the three ecotypes defined by Ikeda *et al.* (2017). The garden consisted of over 4000 cuttings planted in four replicated blocks with 2 m of spacing and has previously been described (Cooper *et al.*, 2019; Hultine *et al.*, 2020a). Mean annual temperature in the garden was 22.8°C, and mean annual daily maximum temperature (MAMT) was 31.6°C (PRISM Climate Group, 2022). The garden was regularly watered from flood irrigation delivered from a nearby reservoir with a centrifugal pump.

We selected eight populations from the Sonoran Desert ecotype for study. The exclusive selection of genotypes within the Sonoran Desert ecotype allowed us to evaluate local adaptation to heat stress within (1) the warmest region of *P. fremontii's* distribution, (2) within a single river network, and (3) within a distinct genetic group (Cushman *et al.*, 2014). The elevation of the source population sites ranged from 70 m asl to 1234 m asl (Table 1; Fig. 2) and transfer distance – defined as the difference between the MAMT of the common garden location and the MAMT of population source location (Grady *et al.*, 2011) – ranged from 1.06°C to 6.32°C (Table 1). Herein, each population is labeled by its transfer distance. A single replicate of 10 genotypes per population ($n = 80$ genotypes) was haphazardly selected for study. To minimize potential confounding microsite effects within the common garden, all of the genotypes were selected within only two of the four blocks, and individual genotypes occurring along the edge of each block were avoided. At the onset of the study in May, mean population diameter at the root crown ranged from 31.3 mm (±1.8 SE) to 61.7 mm (±4.7 SE), and mean population tree height ranged from 2.12 m (±0.14 SE) to 4.62 m (±4.62 SE; Table 1). Diameter at the root crown and tree height was both negatively correlated with transfer distance, that is the largest trees generally came from populations with the lowest transfer distance (Supporting Information Fig. S1). Two field campaigns were conducted during the 2021 growing season to evaluate leaf thermal tolerance, leaf-level stomatal conductance, leaf temperature, leaf water potential, leaf turgor loss point, and leaf morphology (to be described later for measurement details). The first campaign was conducted from 3 May to 6 May (Day of year 123–126) when maximum daytime air temperatures are typically below 35°C. The second campaign occurred from 20 August to 22 August (Day of year 232–234) when historic air temperatures often exceed 45°C. An Onset Hobo micrometeorological station (Onset Inc., Bourne, MA, USA) was installed in an open area in the common garden and measured air temperature (T_{air}: °C), humidity (η_h: %), and photosynthetic actively radiation (Q: μmol m^{-2} s^{-1}) from 3 May 2021 to 23 August 2021 every 30 s with mean values recorded every 10 min. Measurements of temperature and humidity were used to calculate atmospheric vapor pressure deficit (D: kPa) from Monteith & Unsworth (1990).

Field leaf collections

In mid-July, 2022, leaves were collected from all eight *P. fremontii* source population locations to measure T_{crit}, and Ψ_{TLP} for comparison with values measured in the common garden. It was not possible to collect leaves from all of the same source genotypes as those that comprised the common garden due to mortality from fire and flooding of some genotypes since

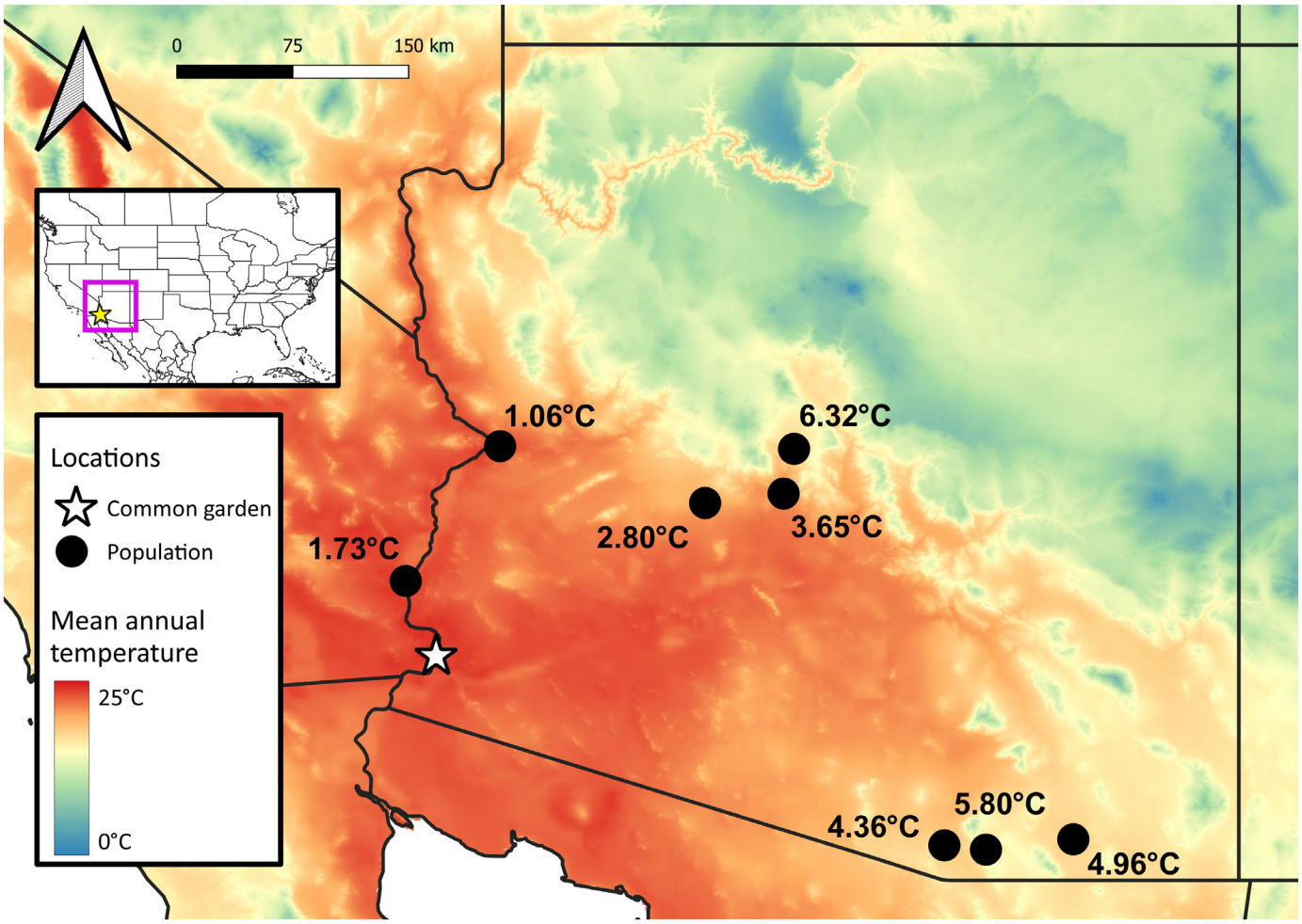

Fig. 2 Source location for the Yuma common garden and the eight source population locations for *Populus fremontii*. Transfer distances are displayed next to each icon and were calculated using the mean annual maximum temperatures at each location between 1991 and 2020 (PRISM Climate Group, 2022). Mean annual temperature data acquired from Fick & Hijmans (2017). For details of the source population locations, see Table 1.

Table 1 River/creek system, site elevation, mean annual maximum daily temperature (MAMT), transfer distance, latitude and longitude of source populations, basal stem diameter, and tree height of genotypes studied in an experimental common garden in Yuma, AZ, USA.

River/Creek	Site elevation (m)	MAMT (°C)	Transfer distance (°C)	Lat	Long	Basal stem dia (mm)	Tree height (m)
Colorado River	70	29.83	1.73	33.362	−114.698	53.5 (5.5)	3.80 (0.39)
Bill Williams River	143	30.50	1.06	34.276	−114.059	61.7 (4.7)	4.62 (0.25)
Hassayampa River	575	28.76	2.80	33.909	−112.676	49.5 (4.1)	3.54 (0.26)
New River	666	27.91	3.65	33.948	−112.136	38.0 (2.6)	2.70 (0.15)
Santa Cruz River	986	27.20	4.36	31.565	−111.045	37.7 (2.4)	2.42 (0.10)
Agua Fria	988	25.23	6.32	34.257	−112.066	36.9 (3.7)	2.92 (0.31)
San Pedro River	1219	26.60	4.96	31.610	−110.167	31.3 (1.8)	2.12 (0.14)
Sonoita Creek	1234	25.76	5.80	31.536	−110.763	46.5 (1.8)	3.11 (0.14)

Numbers in parentheses represent ± SE of the means.

the original collections in 2013. However, we were able to collect leaves from co-occurring trees at all locations. Although *P. fremontii* individuals are rarely clonal (Schweitzer *et al.*, 2002), leaves were collected from trees that were at least 10 m apart at each location. A pole pruner was used to collect 10–20 fully expanded sunlit leaves, typically from canopy heights ranging from 6.0 to 7.0 m (Table S1). The leaves were then processed according to methods described below. The maximum air temperature (T_{smax}) experienced at each field location between 2012 and 2021 was extracted from publicly available meteorological

data from nearby weather stations. The maximum distance between collections sites and the nearest weather station was 10 km with a difference in elevation of 130 m. Data were used to calculate field thermal safety margins defined as $T_{crit}-T_{smax}$ (O'Sullivan *et al.*, 2017).

Measurements of leaf thermal tolerance

Leaf thermal tolerance was quantified by measuring minimum chlorophyll *a* fluorescence (F_o) in leaf samples across a steady temperature gradient. The thermal sensitivity of F_o was measured with a Closed FC-800-C FluorCam fluorescence imager coupled to a TR2000 thermoregulator (Photon System Instruments, Drasov, Czech Republic). Three, recently flushed, sunlit leaves were collected from each genotype in mid-to-late afternoon and immediately placed in a dark cooler and shipped from Yuma or driven from field locations to the laboratory where they were stored in a refrigerator before processing. Because *P. fremontii* continue to flush leaves throughout the growing season, recently flushed leaves selected in August were likely of a similar age as leaves selected in May. Before measuring the thermal sensitivity of F_o, one leaf from each genotype was randomly selected to evaluate the maximum quantum yield of PSII to confirm that the leaves maintained a high photochemical quenching capacity between the time they were collected and the time they were analyzed (usually < 72 h). Maximum quantum yield was defined as $F_v : F_m$, where F_m is the maximum fluorescence yield and $F_v = F_m - F_o$ (Maxwell & Johnson, 2000). Leaves were dark adapted for 30 min and then exposed to an initial 30 µs initial light pulse to determine F_o, followed by a 2400 µmol m^{-2} s^{-1} saturating light pulse to determine F_m. Leaves with values above 0.70 (unitless) were considered healthy enough to measure thermal sensitivity of F_o, given that 0.70 and above is near the theoretical optimum of 0.83 (Maxwell & Johnson, 2000).

For F_o thermal sensitivity measurements, three 5.5 mm diameter disks were sectioned from the central part of each leaf, taking care to avoid major leaf veins. The leaf disks were placed with deionized water into wells of a heating block apparatus coupled to the TR2000 thermal regulator. The heating block was then placed inside of the FC-800-C FluorCam enclosure for 30 min. After the leaves were dark adapted, F_o was measured every 30 s as the heating block temperature was raised from 30°C to 60°C at a rate of 0.5°C/1 min. Each F_o measurement was taken in five rapid bursts of far-red light that occurred over 160 ms. The F_o values collected during each of these five bursts were averaged to give a single value per temperature point.

Measurements of leaf thermal regulation

Leaf stomatal conductance (g_s, mol m^{-2} s^{-1}) was measured with a LI600 Porometer (LiCor Inc., Lincoln, NE, USA). Measurements were conducted on three, recently flushed, fully expanded leaves per genotype in both May and August. Each leaf was positioned *c.* 1.5–2 m above the ground surface. In both May and August, measurements were conducted at mid-morning (*c.* 9:00 h–10:45 h), midday (*c.* 12:00 h–13:45 h), and mid-afternoon (*c.* 15:00 h–16:45 h) on the same leaves during each measurement period. In some cases, the selected leaves were shaded during one or more measurement period, and when possible, a different nearby leaf was selected on the same genotype. Because *P. fremontii* leaves are amphistomatous (Blasini *et al.*, 2021), measurements were made on both sides of each leaf to calculate an average leaf g_s. Due to the LI600's open chamber design, the environmental conditions in the chamber were matched to the local ambient conditions.

Leaf temperatures (T_{leaf}, °C) were determined simultaneously with measurements of g_s using an infrared thermal imaging camera for smartphones (FLIR One Pro; Teledyne FLIR Inc., Wilsonville, OR, USA). Thermal images were processed using FLIR Thermal Studio Pro (Teledyne FLIR Inc.) to extract mean T_{leaf}. Each leaf was outlined with a polygon tool within FLIR Thermal Studio Pro and the average maximum leaf temperature was extracted from all of the pixels within the polygon.

Measurements of leaf hydraulic safety and structure

Leaf water potentials were measured on all 80 genotypes in May and August. Measurements were conducted at predawn (Ψ_{pd}, MPa) between 3:00 h and 5:00 h, and during the day between 11:00 h and 13:00 h and between 15:00 h and 17:00 h to determine minimum daytime water potentials (Ψ_{min}, MPa). During each measurement period, a single, open canopy leaf was excised with a sharp razor blade at *c.* 1.5 m above the ground surface. The excised leaves were immediately placed in a sealed ziploc containing a moist paper towel and placed in a dark cooler. All water potential measurements were conducted within 15 min of collection using a 1505XD-EXP Scholander type pressure chamber (PMS Instruments, Albany, OR, USA).

Leaf turgor loss point (Ψ_{TLP}) was measured as a predictor of leaf hydraulic limits because (1) it is a strongly correlated with aridity within and across biomes (Bartlett *et al.*, 2012b), (2) strongly predicts the leaf water potential at which stem and leaf hydraulic conductance falls to 50% of maximum (Blackman *et al.*, 2010; Bartlett *et al.*, 2016), and (3) strongly predicts the leaf water potential that induces a 50% decrease in stomatal conductance (Bartlett *et al.*, 2016). Small sun exposed twigs were excised and the cut ends were immediately submerged in water in a sealed cooler and transported to the laboratory where the stems were covered with a plastic bag and placed in a refrigerator. Three fully hydrated leaves were removed from the stem the following morning, and the petioles were excised with a razor blade, and any surface moisture, if present, was removed. A 7.25 mm diameter cork-borer was used to cut two disks out from each fresh leaf, one on each side of the leaf approximately midpoint between the mid-rib and the outer edge of the leaf, but avoiding any large veins. The leaf disks were quickly sealed in aluminum foil and submerged into liquid nitrogen for *c.* 5 min, after which 5–10 small holes were punctured randomly throughout the disk using a sharp-tipped tweezers. The leaf disks were placed in a calibrated VAPRO 5520 vapor pressure osmometer (Wescor Inc., Logan, UT, USA) to measure the leaf osmotic potential at full turgor ($\Psi_{\pi 100}$, MPa). We used the regression equation from Bartlett

et al. (2012a) to calculate turgor loss point as $\Psi_{TLP} = 0.832\Psi_{\pi 100} - 0.631$.

In order to validate the osmometer approach to measure Ψ_{TLP}, we compared Ψ_{TLP} values obtained from the osmometer with Ψ_{TLP} values obtained from standard pressure volume curves (Schulte & Hinckley, 1985). Sunlit, *P. fremontii* leaves were collected over a 1-wk period in October, 2022, from a single tree and split into two groups with Ψ_{TLP} measured with the osmometer in one group and Ψ_{TLP} measured using pressure–volume curves in the second group.

Statistical analyses

All statistical analyses were performed in either R v.4.1.2 (R Core Team, 2019) or PRISM v.9.4.1 (GRAPHPAD Software, LLC, Boston, MA, USA). Breakpoint regression was used to calculate T_{crit}, the temperature associated with the inflection point between the slow- and fast-rise phase of the temperature-F_o response (See Fig. S2 for an example of the temperature-F_o response curve), using the SEGMENTED package in R (Muggeo, 2017). Before calculating T_{crit}, mean genotype F_o values for each sampling period and location were scaled to fall between 0 and 1, where 0 was the minimum recorded F_o and 1 was the maximum recorded F_o. Using this transformed data, T_{crit} was calculated for each disk following procedures from Arnold *et al.* (2021), which were modified to account for a difference in instruments used and data output format.

Before analyzing the data, we examined whether each variable met the assumptions of normality and homogeneity of variance, using a Shapiro or Bartlett test. In cases where the data were not normally distributed, they were normalized by log transformation. Once the requirements of normality were met, relationships between physiological traits including: T_{crit}, g_{smin}, ΔT_{leaf}, Ψ_{pd}, Ψ_{min}, Ψ_{TLP}, Ψ_s, and transfer distance were analyzed using linear regression. Differences in T_{crit} and Ψ_{TLP} among measurements conducted in May and August at the common garden and from field locations were evaluated using analysis of variance (ANOVA). When a trait showed significant variation, we used a Tukey's HSD *post hoc* test to detect difference among groups. Differences in trait means between May and August at the common garden were evaluated using a paired student's *t*-test with equal variance. For all tests, only *P*-values of < 0.05 were considered significant.

Results

Weather conditions at the common garden

Between 3 May (commencement of first field campaign) and 21 August (conclusion of second field campaign), the mean daily maximum temperature at the common garden was 39.60°C, ranging from 28.49°C on 21 May (Day of year 141) to 45.44°C on 16 June (Day 166; Fig. S2a). The mean daily minimum temperature was 20.01°C, ranging from 7.22°C on 21 May (Day 166) to 28.89°C on 12 July (Day 193; Fig. S3a). On average, *D* peaked at 5.55 kPa, ranging from 3.00 kPa on 24 July (Day 205) to 8.51 kPa on 15 June (Day 166; Fig. S3b). Mean diurnal low *D* was 0.70 kPa, ranging from 0.14 kPa on 24 May (Day 144) to 1.66 kPa on 12 July (Day 193; Fig. S3b). Daytime *Q* was above 2000 µmol m^{-2} s^{-1} on virtually every day except 24 July (Day 205, Data not shown), reflecting the near constant sunlight that the Yuma area receives throughout the year.

Leaf thermal tolerance

In May, mean T_{crit} among all genotypes was 48.85°C (±0.13 SE) and, in August, increased to 50.06°C (±0.09 SE), while at the native field sites in mid-July, mean T_{crit} was 51.37°C (±0.11 SE). Seasonal differences in T_{crit} at the common garden were highly significant ($P < 0.0001$, Fig. 3a), as were differences between May and August with leaves collected from the field locations ($P < 0.0001$, Fig. 3a). In May, T_{crit} was negatively correlated with transfer distance (Table 2). However, transfer distance only constrained 6% in the variation in T_{crit} of all genotypes. Counter to Hypothesis 1, no relationship was detected between T_{crit} and transfer distance in either August (Table 2), or from the native field locations (data not shown).

The mean T_{crit} of 51.37°C of all genotypes from the field locations was higher than 87% of T_{crit} levels in over 170 species recently analyzed and published in O'Sullivan *et al.* (2017; Fig. S4). However, when compared to maximum summer heat wave levels reached over the last 10 yr (2012–2021), mean thermal safety margins ($T_{crit} - T_{smax}$) ranged from −0.51°C warmest location (Transfer Distance = 1.06°C) to 11.25°C at the coolest location (TD = 6.32°C; Fig. 3b,c). Moreover, an increase in predicted summertime temperatures of 1.9°C, and 5.0°C by 2050 and 2100, respectively (Cayan *et al.*, 2013), would result in negative thermal safety margins during the warmest heat waves in up to four of the eight populations analyzed (Fig. 3b,c), assuming that increases in mean annual summer temperatures reflect increases in maximum heat wave conditions.

Leaf thermoregulation

No relationship was detected between May g_{smin} and transfer distance (Table 2; Fig. 4a). Mean air temperature in May was 34.80°C and ranged from 32.15°C to 36.99°C during periods in which maximum leaf temperatures were measured. Afternoon ΔT_{leaf} of all genotypes was on average 3.76°C. However, no trend was detected between ΔT_{leaf} and transfer distance (Table 2; Fig. 4b).

In August, mean g_{smin} was 0.226 mol m^{-2} s^{-1} (±0.03 SE): nearly twofold above g_{smin} measured in May (Table 2), even though mean afternoon *D* was virtually equal between the two periods (4.88 kPa in May vs 4.85 kPa in August). In contrast to May, g_{smin} measured in August decreased with transfer distance (Table 2; Fig. 4c), supporting Hypothesis 2. Transfer distance accounted for 20% of the variation in g_{smin} at the individual genotype level ($F_{1,74} = 18.43$, $P < 0.0001$, Table 2; Fig. 4c). Contrasts in g_{smin} between May and August (i.e. August g_{smin} − May g_{smin}) were also inversely correlated with transfer distance,

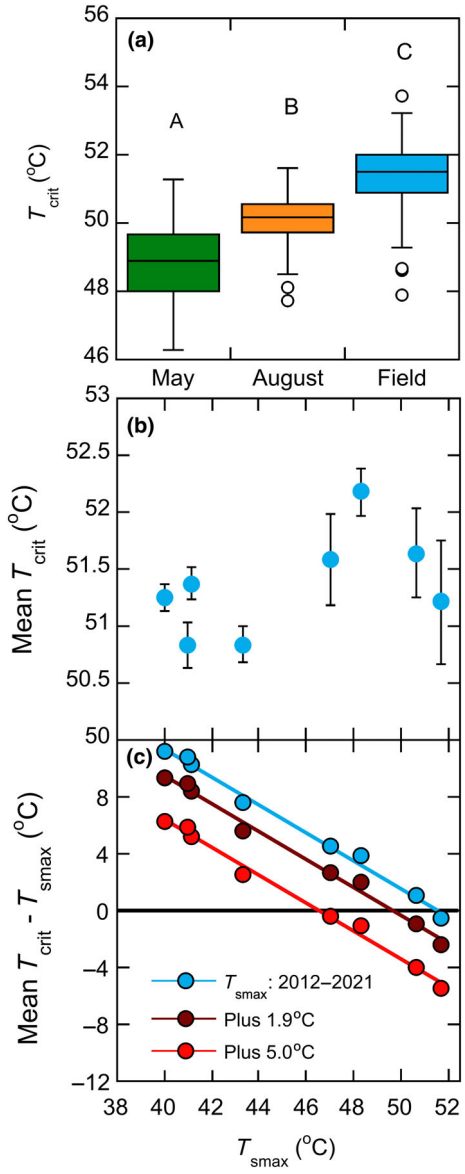

Fig. 3 Thermal tolerance (T_{crit}) and Thermal safety margins (T_{crit}–T_{smax}) in *Populus fremontii* leaves collected from an experimental common garden and at population source locations in Arizona. (a) Box and whisker plot showing patterns of leaf T_{crit} in *Populus fremontii* genotypes measured in a common garden in Yuma, Arizona from leaves collected in May 2021 and August 2021, and from leaves collected from genotypes at the source locations in the lower Colorado River Basin. The box and whisker plots show the median, 25th and 75th percentiles (boxes), and the 10th and 90th percentiles (error bars). Different letters represent significant differences among the different leaf groups ($P < 0.05$). (b) Mean T_{crit} in relationship to maximum temperature measured at each location between 2012 and 2021 (T_{smax}). Error bars represent the SE of the means ($n = 10$ genotypes per population). (c) Mean T_{crit}–T_{smax} in relationship to T_{smax} measured between 2012 and 2021, and with predicted increases in regional mean annual temperatures by 2050 (1.9°C) and 2100 (5.0°C; Cayan *et al.*, 2013).

with transfer distance accounting for 26% of the variation at the genotype level ($F_{1,74} = 25.42$, $P < 0.0001$, Fig. 4e).

Mean air temperature during periods in which maximum leaf temperatures were measured was 2.66°C warmer in August than in May, ranging from 35.82°C to 39.01°C. Afternoon ΔT_{leaf} of all genotypes was on average 1.31°C cooler than air temperature, and unlike in May, there was a fairly robust correlation between transfer difference and ΔT_{leaf} at the genotype level ($R^2 = 0.29$, $F_{1,79} = 30.08$, $P < 0.0001$, Table 2; Fig. 4d), supporting Hypothesis 3. Mean ΔT_{leaf} decreased at least 3.18°C in all populations from May to August, but was particularly striking in the population with the lowest transfer distance (1.06°C) where mean ΔT_{leaf} decreased 9.28°C (Fig. 4f).

There was a fairly robust inverse relationship between ΔT_{leaf} and g_{smin} across all genotypes and both measurements periods with the log(g_{smin}) accounting for 38% of the variation in ΔT_{leaf} ($F_{1,152} = 93.9$, $P < 0.0001$, Fig. S5).

Hydraulic safety and leaf structure

Mean Ψ_{pd} from all genotypes was nearly identical between May and August (Table 2; Fig. S6), indicating that soil water availability was similar during both periods. In May, mean Ψ_{pd} of all genotypes was −0.37 (±0.02 SE) while in August, mean Ψ_{pd} was −0.38 (±0.01 SE; Table 2). There was no relationship between Ψ_{pd} and transfer distance in either May or August (Table 2). In May, mean Ψ_{min} was −1.86 MPa (±0.03 SE), with no relationship detected between Ψ_{min} and transfer distance (Table 2). Mean Ψ_{min} in August was −1.92 MPa (±0.03 SE): nearly identical to Ψ_{min} measured in May (Table 2; Fig. S6). Again, there was no relationship between Ψ_{min} and transfer distance (Table 2).

A comparison between the osmometer and the pressure–volume curve approach to measure Ψ_{TLP} in *P. fremontii* yielded no differences between methods. Mean Ψ_{TLP} was −2.69 MPa (±0.05 SE, $n = 10$ leaves), and −2.61 MPa (±0.12 SE, $n = 13$ leaves), from the osmometer and from pressure–volume curves, respectively ($t = 0.60$, $P = 0.56$, data not shown). In May, mean leaf Ψ_{TLP} among all genotypes was −2.55 MPa (±0.02 SE), and no relationship was detected between Ψ_{TLP} and transfer distance (Table 2; Fig. 5a). In August, Ψ_{TLP} was similar to May with a mean among all genotypes of −2.59 MPa (±0.02 SE). However, unlike in May, Ψ_{TLP} increased slightly (i.e. became less negative) with transfer distance, although the regression only captured 10% of the variation in Ψ_{TLP} (Table 2, Fig. 5b).

In May and August, the hydraulic safety margin (Ψ_s: i.e. Ψ_{TLP}–Ψ_{min}) was a fairly robust −0.69 MPa (±0.03 SE), and −0.60 MPa (±0.03 SE), respectively (Table 2). No relationship was detected between Ψ_s and transfer distance in either May or August (Table 2).

In contrast to patterns of Ψ_{TLP} measured in the common garden, there was a fairly robust relationship between Ψ_{TLP} and transfer distance in field-collected leaves (Fig. 5c), with warm-adapted genotypes having lower mean Ψ_{TLP} values, supporting Hypothesis 4. Among all genotypes, transfer distance captured 30% of the variation in Ψ_{TLP} (Fig. 5c). In particular, genotypes from the warmest location (1.06°C) had the largest departure in Ψ_{TLP} from values measured at the common garden, with a population mean of −2.89 MPa (±0.02 SE) at the field location compared with mean values of −2.59 MPa (±0.07 SE) and

Table 2 Leaf thermal tolerance (T_{crit}), minimum daytime stomatal conductance (g_{smin}), difference between maximum leaf temperature and air temperature (ΔT_{leaf}), predawn leaf water potential (Ψ_{leaf}), minimum daytime leaf water potential (Ψ_{min}), leaf turgor loss point (Ψ_{TLP}), and hydraulic safety margin (Ψ_s) from *Populus fremontii* leaves measured in May and August at an experimental common garden in Yuma, AZ, USA.

	May				August			
Measurement	Genotype mean	High population mean	Low population mean	*F* statistic	Genotype mean	High population mean	Low population mean	*F* statistic
T_{crit} (°C)	48.85 (0.13)	50.12 (0.20): *1.73°C*	47.91 (0.27): *3.65°C*	**4.92***	50.06 (0.09)	51.60 (0.23): *1.73°C*	49.48 (0.25): *3.65°C*	0.99
g_{smin} (mol m^{-2} s^{-1})	0.119 (0.003)	0.148 (0.008): *4.95°C*	0.093 (0.010): *1.06°C*	3.31	0.226 (0.009)	0.329 (0.026): *1.73°C*	0.148 (0.023): *6.32°C*	**18.43*****
ΔT_{leaf} (°C)	3.76 (0.25)	6.02 (0.55): *1.06°C*	2.59 (0.63): *6.32°C*	2.52	−1.31 (0.20)	0.06 (0.10): *3.65°C*	−3.27 (0.54): *1.06°C*	**30.08*****
Ψ_{pd} (MPa)	−0.37 (0.02)	−0.26 (0.01): *4.35°C*	−0.58 (0.05): *2.80°C*	0.13	−0.38 (0.01)	−0.30 (0.01): *4.35°C*	−0.46 (0.02): *1.06°C*	1.98
Ψ_{min} (MPa)	−1.86 (0.03)	−1.75 (0.05): *5.78°C*	−2.01 (0.09): *3.65°C*	0.07	−1.92 (0.03)	−1.85 (0.10): *4.95°C*	−2.12 (0.06): *2.80°C*	0.05
Ψ_{TLP} (MPa)	−2.55 (0.02)	−2.45 (0.02): *4.35°C*	−2.64 (0.03): *5.78°C*	0.77	−2.59 (0.02)	−2.50 (0.02): *4.35°C*	−2.70 (0.02): *1.73°C*	**9.10***
Ψ_s (MPa)	−0.69 (0.03)	−0.50 (0.09): *3.65°C*	−0.90 (0.06): *5.78°C*	0.03	−0.60 (0.03)	−0.43 (0.07): *2.80°C*	−0.76 (0.07): *1.73°C*	1.01

Numbers in parentheses represent ± SE of the means. Numbers in italics represent the transfer distance of the source population (See Table 1). 'High' and 'Low' population means indicate the population that expressed the highest and lowest mean values, respectively, for a given trait. *F* statistics shown in bold represent significant relationships ($P < 0.05$) between the parameter and transfer distance. *, $P < 0.05$; ***, $P < 0.0001$.

−2.64 MPa (±0.02 SE) in May and August, respectively (Fig. 5).

Discussion

Overall findings

Results from this investigation yielded two overarching findings. First, despite having a higher leaf thermal tolerance relative to most species, *Populus fremontii* trees along the hyper-arid lower Colorado River still face a limited, and in some locations, a potentially disappearing thermal safety margin (Fig. 3), without significant leaf cooling in midsummer. Second, under well-watered conditions, *P. fremontii* genotypes from the warmest edge of its distribution maintain cooler leaves during the warmest periods of the year as a consequence of expressing a higher midday leaf conductance relative to genotypes from more temperate locations (Fig. 4). Coupled with achieving a relatively high drought tolerance, reflected in leaves having a lower Ψ_{TLP} (Fig. 5), warm-adapted genotypes may be able to withstand some of the most extreme heat waves predicted for the lower Colorado River corridor as long as *P. fremontii* roots remain connected to the water table. However, declining river flows that have fallen dramatically below historic levels due to over-allocation of river water and over two decades of drought could lower water tables along the lower Colorado River. Even a partial decoupling of *P. fremontii* roots during extreme heat wave events could result in leaf temperatures rising above thermal thresholds that in turn, could trigger widespread *P. fremontii* mortality events (e.g. Fig. 1) in a region where *P. fremontii* gallery forests provide a critical thermal refuge for threatened plant and animal taxa.

Leaf thermal tolerance

Leaf thermal tolerance at the common garden increased from May to August as canopies were exposed to temperatures that exceeded 45°C in early summer. Previous research has shown that T_{crit} can be exceptionally plastic with increases being reported in common wheat of over 2°C from sunrise to solar noon during a single day (Posch *et al.*, 2022). Large temporal variations in leaf thermal tolerance are likely related to rapid acclimation to heat exposure caused by the induction of heat shock proteins, the accumulation of antioxidant enzymes, and/or changes in cell membrane function and chemistry (Seemann *et al.*, 1986; Knight & Ackerly, 2003; Hüve *et al.*, 2006, 2011; Khan & Shashwar, 2020). Exposure to heat stress can trigger the rapid expression of genes that up-regulate heat shock protein induction in ways that are ubiquitous across organisms (Khan & Shashwar, 2020). Therefore, potential rapid acclimation in leaf thermal tolerance may explain why T_{crit} not only increased from May to August, but why there was no clear relationship between T_{crit} and transfer distance since all genotypes in the common garden were exposed to the same level of heat stress.

Interestingly, leaf thermal tolerance of leaves collected at the field locations was also not correlated with the mean annual daily maximum temperature (counter to Hypothesis 1). Instead, mean population T_{crit} values were at or above 50.84°C, putting *P. fremontii* among the most thermally tolerant tree species measured to date – regardless of location of source population – compared with other woody taxa and locations (O'Sullivan *et al.*, 2017). One plausible explanation for the higher-than-expected thermal tolerance based on transfer distance would be that all of the source sites experienced unusually high growing season temperatures in 2022 before when the leaves were

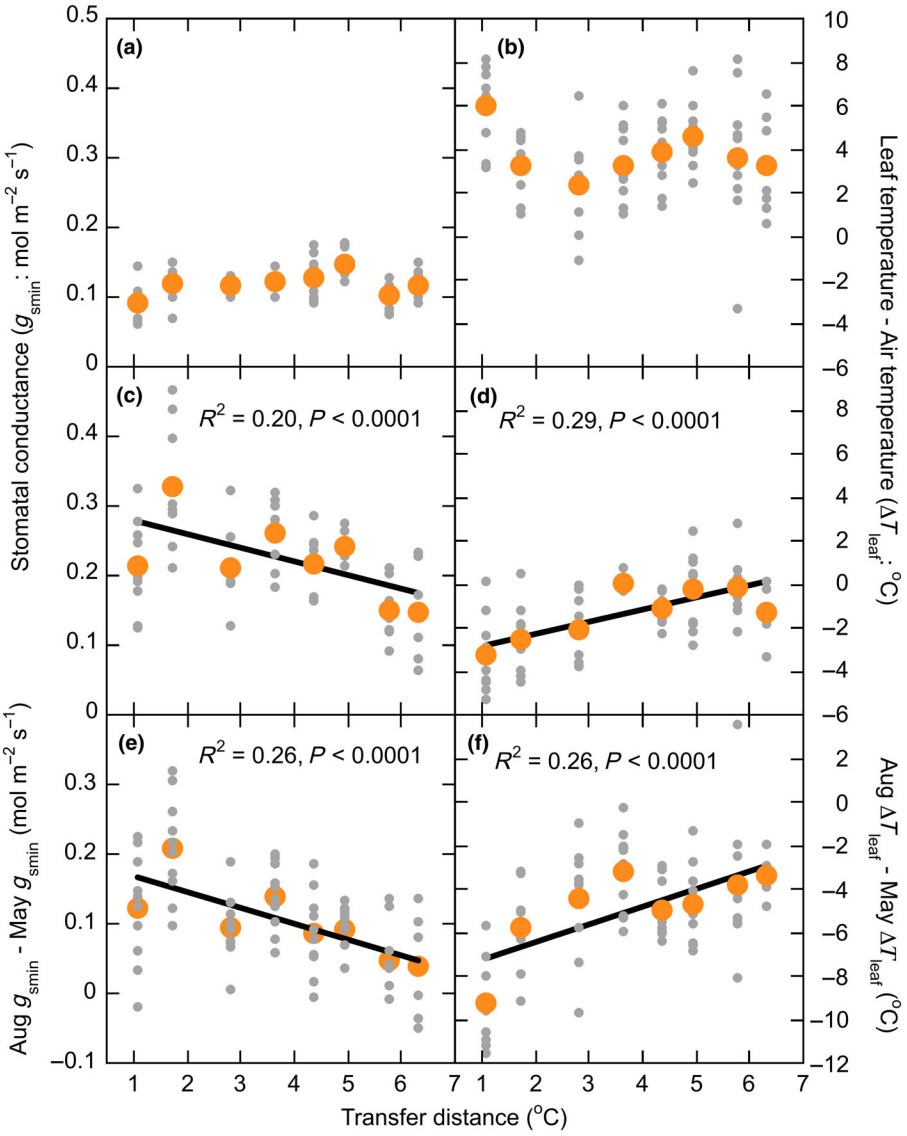

Fig. 4 Minimum daytime stomatal conductance (g_{smin}) and maximum leaf temperature subtracted from air temperature (ΔT_{leaf}) in relation to transfer distance measured on sun leaves of *Populus fremontii* genotypes in May and August 2021 at an experimental common garden near Yuma, AZ, USA. (a) Stomatal conductance measured in May, (b) leaf temperature measured in May, (c) stomatal conductance measured in August, and (d) leaf temperature measured in August. (e) Differences between g_{smin} in August and g_{smin} in May. (f) Difference between Δ_t in August and Δ_t in May. Large orange symbols represent the population means and small grey symbols represent values from individual genotypes.

analyzed. However, maximum air temperatures before leaf collections ranged by 9.50°C, from 37.22°C to 46.72°C, indicating that strong contrasts in heat exposure were present among sites. One previous study also found no relationship between leaf T_{crit} in wheat and latitude of origin (Posch *et al.*, 2022).

Despite achieving a relatively high leaf thermal tolerance, air temperatures along the lower Colorado River may be exceeding the thermal limits of leaf metabolism in *P. fremontii* trees. For example, the population with the lowest transfer distance, occurring along the lower Bill Williams River at its confluence with the Colorado River, has experienced summer air temperatures that have often exceeded 50°C, over the last decade, including reaching a high of 51.72°C in 2017. This stand has also experienced extensive recent mortality of over 85% over the last decade, likely as a consequence of lowering water tables and heat waves (Whitham *et al.*, 2020; Cooper *et al.*, 2022). The maximum summer temperatures at this location have exceeded the thermal limits of *P. fremontii* trees, based on mean T_{crit} measured from this site (Fig. 3). If we assume that expected regional increases in summer temperatures reflect average increases in maximum growing season temperatures, then it is plausible that heat waves could exceed measured T_{crit} by over 5°C by the end of the century along the lower Bill Williams River. Although caution should be used when trying to predict the intensity of future heat waves from down-scaled climate models (Tapiador *et al.*, 2020), data indicate that the thermal limits of leaf metabolism may be far exceeded in many *P. fremontii* stands along the already hyper-arid lower Colorado River corridor without sufficient water for transpirational cooling.

Leaf thermal regulation and hydraulic safety

In the present study, all of the populations in the common garden had leaf afternoon temperatures that were above air temperature in May, but switched in August with leaf temperatures that fell below air temperatures, even though air temperatures were

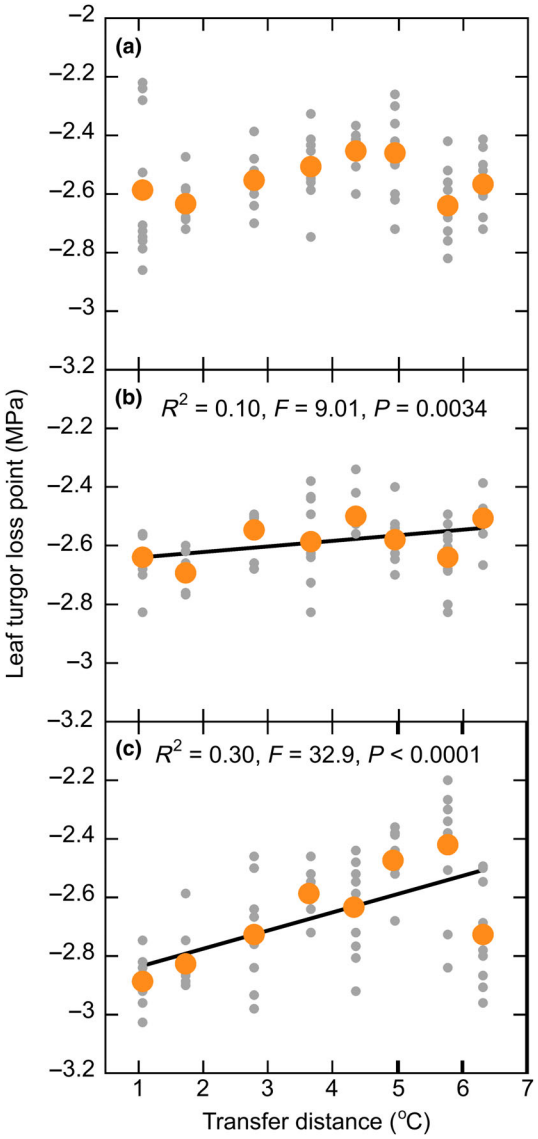

Fig. 5 Relationship between leaf turgor loss point and population transfer distance measured in May (a) and August 2021 (b) on *Populus fremontii* genotypes measured at an experimental common garden near Yuma, AZ, USA. Panel (c) shows the relationship between leaf turgor loss point and population transfer distance measured on leaves collected in July 2022 from the population source locations in Arizona. Large orange symbols represent the population means and small grey symbols represent values from individual genotypes.

c. 3°C warmer in August, and vapor pressure deficits were similar between months. This seasonal megathermy to homeothermy behavior was especially prevalent in populations with the smallest transfer distances (Fig. 4) that had the most similar climate conditions as the common garden. In particular, the population with the lowest transfer distance (i.e. from the Bill Williams River) where mean leaf temperatures relative to air temperature dropped by 10°C from May to August. Seasonal decreases in leaf temperature corresponded with increases in afternoon stomatal conductance from May to August that were again most prevalent in populations with the lowest transfer distance. Seasonal increases in g_s corroborates sap-flux-scaled stomatal conductance data collected on *P. fremontii* genotypes from another common garden study. In the previous study, whole-canopy stomatal conductance progressively increased in the warm-adapted genotypes throughout the growing season in response to warmer air temperatures (Blasini *et al.*, 2022). Taken together, results suggest that transpirational leaf cooling is an important adaptive strategy expressed by warm-adapted *P. fremontii* genotypes in response to thermal stress.

In warm environments, leaf homeothermy (i.e. transpirational cooling of T_{leaf} below T_{air}) should not only cool leaves below a lethal threshold, but should also maximize growth and fitness by maintaining net photosynthetic rates near its thermal optimum (Mahon & Upchurch, 1988; Michaletz *et al.*, 2016; Blonder & Michaletz., 2018). However, the extent that homeothermy behavior occurs across species and biomes remains an open question (Drake *et al.*, 2020; Yi *et al.*, 2020; Still *et al.*, 2022). Presumably, homeothermy behavior is limited to plants that are well watered, but even in well-watered environments, species and genotypes may exhibit a wide range of leaf thermal regulatory strategies depending on plant hydraulic trait expression, stomatal behavior and leaf morphology (Leigh *et al.*, 2017; Fauset *et al.*, 2018; Aparecido *et al.*, 2020; Blasini *et al.*, 2022). In the present study, all of the genotypes were well watered, demonstrated by the high Ψ_{pd} values in both May and August. Yet, differences in mean g_{smin} emerged among populations in ways that likely underpinned cooler leaf temperatures in midsummer, and presumably improved leaf carbon balance over populations having a lower g_{smin} and higher leaf temperatures. The higher growth rates detected in the warmest-adapted genotypes (Fig. S1) were likely a reflection of their capacity to maintain a higher g_{smin} and cooler daytime leaf temperatures, coupled with previous studies showing that these populations also leaf out earlier and set bud later in the year relative to genotypes from cooler locations (Cooper *et al.*, 2019, 2022; Blasini *et al.*, 2021).

If all things are equal, maintaining a higher leaf-level g_{smin} comes with the trade-off of either operating with a lower Ψ_{min}, maintaining a higher Huber value (sapwood to leaf area ratio; Tyree & Ewers, 1991), or both. In the present study, no relationship was detected between transfer distance and Ψ_{min}, but in August mean Ψ_{min} among all genotypes were −1.92 MPa (Table 2), or just below the previously reported threshold that induces hydraulic failure, inferred from measurements of xylem cavitation (Li *et al.*, 2008; Choat *et al.*, 2012). However, population mean Ψ_{TLP} measured in the common garden ranged from −2.45 MPa to −2.70 MPa, indicating that all of the genotypes maintained a relatively robust hydraulic safety margin regardless of g_{smin} levels. Likewise, Ψ_{TLP} measured at the host field locations was below −2.80 MPa in the two warmest populations. The relatively low mean Ψ_{TLP} values, and the negative correlation with MAMT, indicate that genotypes from the hyper-arid Colorado River corridor can operate with lower midday water potentials relative to other populations (Fig. 5c), or other *Populus* spp in which Ψ_{TLP} has been reported for Cheung *et al.* (1975), Pezeschki & Hinckley (1988), Braatne *et al.* (1992).

Alternatively, because g_{smin} did not correspond with lower Ψ_{min} in August, it is plausible that warm-adapted genotypes,

instead operated with a higher Huber value, relative to genotypes from cooler areas. A similar common garden study on *P. fremontii* showed that differences in sap-flux-scaled canopy conductance were driven by warm-adapted genotypes maintaining a 36% higher sapwood area to leaf area ratio throughout the growing season (Blasini *et al.*, 2022). Homeostasis in leaf water relations can be achieved via adjustment in Huber values (Carter & White, 2009; Gotsch *et al.*, 2010). However, a reduced leaf area to sapwood area ratio is likely to reduce the whole-plant leaf area ratio (i.e. ratio between total leaf area and total plant biomass; Poorter & Remkes, 1990) in ways that could significantly reduce relative growth rates and fitness (Dijkstra & Lambers, 1986; Cornelissen *et al.*, 1996). Nevertheless, such adjustment may be necessary for *P. fremontii* genotypes to maintain midsummer leaf temperatures below lethal thermal thresholds along the lower Colorado River given current and projected climate conditions.

Ecological implications

Results from this study show that *P. fremontii* is remarkably well adapted to the extreme aridity that persists in the lower Colorado River Basin in terms of leaf thermal tolerance, stomatal regulation and leaf hydraulic function. Yet, recent widespread mortality has occurred along the warm edge of *P. fremontii's* distribution (Whitham *et al.*, 2020; Cooper *et al.*, 2022) in response to marked decreases in soil moisture and increases in evaporative demand (Cayan *et al.*, 2013; Garfin *et al.*, 2013). Over the last two decades, the lower Colorado River corridor as a whole has seen a substantial reduction in vegetation greenness, in part due to increased aridity and drought (Nagler *et al.*, 2021). Although *P. fremontii* can achieve leaf thermal tolerances that are well above most tree taxa, its continued persistence in the lower Colorado River Basin may depend on maintaining groundwater resources and temperature regimes near historic means. Otherwise, *P. fremontii* forests that are of great conservation value because of the critical habitat they provide for diverse biotic communities will continue to be in decline where < 3% of its historic riparian forest extent remains (Noss *et al.*, 1995).

Acknowledgements

This research was supported by the National Science Foundation MacroSystems Biology program (DEB-1340852, DEB-1340856 and DEB-2017895). Special thanks to Debbie and Ken Abbott for additional financial support for this project. We also thank Abraham Cadmus, Isabella De Leon, Julia Gomes, Jessica Guo, Elena Schaefer, Ali Schuessler, and Brett Swihart for their assistance in the field and the laboratory. We acknowledge the helpful technical assistance received from Brad Posch and Andrew Scafaro.

Competing interests

None declared.

Author contributions

MEM and KRH designed the research. MEM, LMTA, DFK and KRH performed the research and analyzed the data. MEM, LMTA, DFK, HFC, CED, CAG, HLT, TGW, GJA and KRH all contributed to the writing and editing of the manuscript.

ORCID

Gerard J. Allan https://orcid.org/0000-0002-8007-4784
Luiza M. T. Aparecido https://orcid.org/0000-0001-8642-6632
Hillary F. Cooper https://orcid.org/0000-0003-2634-1404
Christopher E. Doughty https://orcid.org/0000-0003-3985-7960
Catherine A. Gehring https://orcid.org/0000-0002-9393-9556
Kevin R. Hultine https://orcid.org/0000-0001-9747-6037
Dan F. Koepke https://orcid.org/0009-0008-5728-1655
Heather L. Throop https://orcid.org/0000-0002-7963-4342

Data availability

All genotype-level data of T_{crit}, g_s, m, Ψ_{pd}, Ψ_{min}, and Ψ_{TLP} collected at the common garden in May are available in Dataset S1, and genotype-level data collected in August are available in Dataset S2. All genotype-level data of T_{crit} and Ψ_{TLP} collected at the field locations are available in Dataset S3. The R script used to calculate T_{crit} from breakpoint regression of the relationship between F_o and leaf temperature is available on Github: https://github.com/memoran3/Sample-Tcrit-Extraction.git.

References

Aparecido LML, Woo S, Suazo C, Hultine KR, Blonder B. 2020. High water use in desert plants exposed to extreme heat. *Ecology Letters* **23**: 1189–1200.

Arnold PA, Briceño VF, Gowland KM, Catling AA, Bravo LA, Nicotra AB. 2021. A high- throughput method for measuring critical thermal leaves by chlorophyll imaging fluorescence. *Functional Plant Biology* **48**: 634–646.

Bangert R, Ferrier SM, Evans L, Kennedy K, Grady KC, Hersch-Green E, Allan GJ, Whitham TG. 2013. The proportion of three foundation species and their genotypes influence an arthropod community: restoration implications for the endangered southwestern willow flycatcher. *Restoration Ecology* **21**: 447–456.

Bartlett MK, Klein T, Jansen S, Choat B, Sack L. 2016. The correlations and sequence of plant, stomatal, hydraulic, and wilting responses to drought. *Proceeding of the National Academy of Sciences USA* **113**: 13098–13103.

Bartlett MK, Scoffoni C, Ardy R, Zhang Y, Sun S, Cao K, Sack L. 2012a. Rapid determination of comparative drought tolerance traits: using an osmometer to predict turgor loss point. *Methods in Ecology and Evolution* **3**: 880–888.

Bartlett MK, Scoffoni C, Sack L. 2012b. The determinants of leaf turgor loss point and prediction of drought tolerance of species and biomes: a global meta-analysis. *Ecology Letters* **15**: 393–405.

Bennett KE, Talsma C, Boero R. 2021. Concurrent changes in extreme hydroclimate events in the Colorado River Basin. *Water* **13**: 978.

Blackman CJ, Brodribb TJ, Jordan GJ. 2010. Leaf hydraulic vulnerability is related to conduit dimensions and drought resistance across a diverse range of woody angiosperms. *New Phytologist* **188**: 1113–1123.

Blasini DE, Koepke DF, Bush SE, Allan GJ, Gehring CA, Whitham TG, Day TA, Hultine KR. 2022. Tradeoffs between leaf cooling and hydraulic safety in

a dominant arid land riparian tree species. *Plant, Cell & Environment* **45**: 1664–1681.

Blasini DE, Koepke DF, Grady KC, Allan GJ, Gehring CA, Whitham TG, Cushman SA, Hultine KR. 2021. Adaptive trait syndromes along multiple spectra define cold and warm adapted ecotypes in a widely distributed foundation tree species. *Journal of Ecology* **109**: 1298–1318.

Blonder B, Michaletz S. 2018. A model for leaf temperature decoupling from air temperature. *Agricultural and Forest Meteorology* **262**: 354–360.

Bothwell HM, Keith AR, Cooper HF, Hull JB, Andrews LV, Wehenkel C, Hultine KR, Gehring CA, Cushman SA, Whitham TG *et al.* 2023. Microevoltionary processes in a foundation tree inform macrosystem patterns of community biodiversity and structure. *Forests* **14**: 943.

Braatne JH, Hinckley TM, Stettler RF. 1992. Influence of soil water on the physiological and morphological components of plant water balance in *Populus trichocarpa*, *Populus deltoides* and their F_1 hybrids. *Tree Physiology* **11**: 325–339.

Carter JL, White DA. 2009. Plasticity in the Huber value contributes to homeostasis in leaf water relations of a mallee Eucalypt with variation in groundwater depth. *Tree Physiology* **29**: 1407–1418.

Cayan DM, Tyree KE, Kunkel C, Castro C, Gershunov C, Barsugli J, Ray AJ, Overpeck J, Anderson ML, Russell JL *et al.* 2013. Future climate: projected average. In: Garfin G, Jardine A, Merideth R, Black M, LeRoy S, eds. Assessment of climate change in the Southwest United States*: a report prepared for the national climate assessment. A report by the Southwest Climate Alliance*. Washington, DC, USA: Island Press, 101–125.

Cheung YNS, Tyree MT, Dainty J. 1975. Water relations parameters on single leaves obtained in a pressure bomb and some ecological interpretations. *Canadian Journal of Botany* **53**: 1342–1346.

Choat B, Jansen S, Brodribb TJ, Cochard H, Delzon S, Bhaskar R, Bucci SJ, Feild TS, Gleason SM, Hacke UG *et al.* 2012. Global convergence in the vulnerability of forests to drought. *Nature* **491**: 752–756.

Cooper HF, Best RJ, Andrews LV, Corbin JPM, Garthwaite I, Grady KC, Gehring CA, Hultine KR, Whitham TG, Allan GJ. 2022. Evidence of climate-driven selection on tree traits and trait plasticity across the climate range of a riparian foundation species. *Molecular Ecology* **31**: 5024–5040.

Cooper HF, Grady KC, Cowan JA, Best RJ, Allan GJ, Whitham TG. 2019. Genotypic variation in phenological plasticity: reciprocal common gardens reveal adaptive responses to warmer springs but not to fall frost. *Global Change Biology* **25**: 187–200.

Cornelissen JHC, Castro-Diez P, Hunt R. 1996. Seedling growth, allocation and leaf attributes in a wide range of woody plant species and types. *Journal of Ecology* **84**: 755–765.

Cushman SA, Max T, Meneses N, Evans LM, Ferrier S, Honchak B, Whitham TG, Allan GJ. 2014. Landscape genetic connectivity in a riparian foundation tree is jointly driven by climatic gradients and river networks. *Ecological Applications* **24**: 1000–1014.

Dijkstra P, Lambers H. 1986. Photosynthesis and respiration of two inbred lines of *Plantego major* L. differing in relative growth rate. In: Marcelle R, Clijsters H, Van Poucke M, eds. *Biological control of photosynthesis*. The Hague, the Netherlands: Martinus Nijhoff Publishers, 251–255.

Drake JE, Harwood R, Vårhammar A, Barbour MM, Reich PB, Barton CVM, Tjoelker MG. 2020. No evidence of homeostatic regulation of leaf temperature in *Eucalyptus parramattensis* tree: integration of CO_2 flux and oxygen isotope methodologies. *New Phytologist* **228**: 1511–1523.

Drake JE, Tjoelker MG, Vårhammar A, Medlyn BE, Reich PB, Leigh A, Pfautsch S, Blackman CJ, López R, Aspinwall MJ *et al.* 2018. Trees tolerate an extreme heatwave via sustained transpirational cooling and increased leaf thermal tolerance. *Global Change Biology* **24**: 2390–2402.

Dufresne J-L, Foujols M-A, Denvil S, Caubel A, Marti O, Aumont O, Balkanski Y, Bekki S, Bellenger H, Benshila R *et al.* 2013. Climate change projections using the IPSL- CM5 Earth System Model: from CMIP3 to CMIP5. *Climate Dynamics* **40**: 2123–2165.

Eckenwalder JE. 1977. North American cottonwoods (*Populus*, Salicaceae) of sections Abaso and Aigeiros. *Journal of the Arnold Arboretum* **58**: 193–208.

Fauset S, Freitas HC, Galbraith DR, Sullivan MJP, Aidar MPM, Joly CA, Phillips OL, Viera SA, Gloor MU. 2018. Differences in leaf thermoregulation and water use strategies between three co-occurring Atlantic forest tree species. *Plant, Cell & Environment* **41**: 1618–1631.

Ferrier SM, Bangert RK, Hersch-Green E, Bailey JK, Allan GJ, Whitham TG. 2012. Unique arthropod communities on different host-plant genotypes results in greater arthropod diversity. *Arthropod-Plant Interactions* **6**: 187–195.

Fick SE, Hijmans RJ. 2017. WorldClim 2: new 1km spatial resolution climate surfaces for global land areas. *International Journal of Climatology* **37**: 4302–4315.

Fischer EM, Sippel S, Knutti R. 2021. Increasing probability of record-shattering climate extremes. *Nature Climate Change* **11**: 689–695.

Garfin G, Jardine A, Merideth R, Black M, LeRoy S. 2013. *Assessment of climate change in the southwestern United States: a report prepared for the National Climatic Assessment. A report by the Southwest Climate Alliance*. Washington, DC, USA: Island Press.

Geange SR, Arnold PA, Catling AA, Coast O, Cook AM, Gowland KM, Leigh A, Notarnicola RF, Posch BC, Venn SE *et al.* 2021. The thermal tolerance of photosynthetic tissues: a global systematic review and agenda of future research. *New Phytologist* **229**: 2497–2513.

Gotsch SG, Geiger EL, Franco AC, Goldstein G, Meinzer FC, Hoffmann WA. 2010. Allocation of leaf area and sapwood area affects water relations of co-occurring savanna and forest trees. *Oecologia* **163**: 291–301.

Grady KC, Ferrier SM, Kolb TE, Hart SC, Allan GJ, Whitham TG. 2011. Genetic variation in productivity of foundation species at the edge of their distribution: implications for restoration and assisted migration. *Global Change Biology* **17**: 3724–3735.

Guirguis K, Gershunov A, Cayan DR, Pierce DW. 2018. Heat wave probability in the changing climate of the Southwest US. *Climate Dynamics* **50**: 3853–3864.

Horton JL, Hart SC, Kolb TE. 2003. Physiological condition and water source use of Sonoran Desert riparian trees at the Bill Williams River, Arizona, USA. *Isotopes in Environmental and Health Studies* **39**: 69–82.

Hultine KR, Allan GJ, Blasini D, Bothwell HM, Cadmus A, Cooper HF, Doughty CE, Gehring CA, Gitlin AR, Grady KC *et al.* 2020a. Adaptive capacity in the foundation tree species *Populus fremontii*: implications for resilience to climate change and non-native species invasion in the American Southwest. *Conservation Physiology* **8**: coaa061.

Hultine KR, Bush SE, Ehleringer JR. 2010. Ecophysiology of riparian cottonwood and willow before, during and after two years of groundwater removal. *Ecological Applications* **20**: 347–361.

Hultine KR, Froend R, Blasini D, Bush SE, Karlinski M, Koepke DF. 2020b. Hydraulic traits that buffer deep-rooted plants from changes in hydrology and climate. *Hydrological Processes* **34**: 209–222.

Hüve K, Bichele I, Rasulov B, Niinemets Ü. 2011. When is it too hot for photosynthesis: heat-induced instability of photosynthesis in relation to respiratory burst, cell permeability changes and H_2O_2 formation. *Plant, Cell & Environment* **34**: 113–126.

Hüve K, Bichele I, Tobias M, Niinemets Ü. 2006. Heat sensitivity of photosynthetic electron transport varies during the day due to changes in sugars and osmotic potential. *Plant, Cell & Environment* **29**: 212–228.

Ikeda DH, Max TL, Allan GJ, Lau MK, Shuster SM, Whitham TG. 2017. Genetically informed ecological niche models improve climate change predictions. *Global Change Biology* **23**: 164–176.

Khan Z, Shashwar D. 2020. Role of heat shock proteins (HSPs) and heat stress tolerance in crop plants. In: Roychowdhury R, Choudhury S, Hasanuzzaman M, Srivastava S, eds. *Sustainable agriculture in the era of climate change*. Basel, Switzerland: Springer Nature, 211–234.

Knight CA, Ackerly DD. 2002. An ecological and evolutionary analysis of photosynthetic thermotolerance using the temperature-dependent increase in fluorescence. *Oecologia* **130**: 505–514.

Knight CA, Ackerly DD. 2003. Evolution and plasticity of photosynthetic thermal tolerance, specific leaf area and leaf size: congeneric species from desert and coastal environments. *New Phytologist* **160**: 337–347.

Leigh A, Servanto S, Close JD, Nicotra AB. 2017. The influence of leaf size and shape on thermal dynamics: does theory hold up under natural conditions? *Plant, Cell & Environment* **40**: 237–248.

Li Y, Sperry JS, Taneda H, Bush SE, Hacke UG. 2008. Evaluation of centrifugal methods for measuring xylem cavitation in conifers, diffuse- and ring-porous angiosperms. *New Phytologist* **177**: 558–568.

Mahon JR, Upchurch DR. 1988. Maintenance of constant leaf temperature by plants – I. Hypothesis limited homeothermy. *Environmental and Experimental Botany* **28**: 351–357.

Maxwell K, Johnson GN. 2000. Chlorophyll fluorescence – a practical guide. *Journal of Experimental Botany* **51**: 659–668.

Michaletz ST, Weiser MD, McDowell NG, Zhou J, Kaspari M, Helliker BR, Enquist BJ. 2016. The energetic and carbon economic origins of leaf thermoregulation. *Nature Plants* **2**: 1–9.

Monteith JL, Unsworth MH. 1990. *Principles of environmental physics*. London, UK: Arnold.

Muggeo VMR. 2017. Interval estimation for the breakpoint in segmented regression: a smooth score-based approach. *Australian and New Zealand Journal of Statistics* **59**: 311–322.

Nagler PL, Barreto-Muñoz A, Chavoshi Borujeni S, Nuori H, Jarchow CJ, Didan K. 2021. Riparian area changes in greenness and water use on the lower Colorado River in the USA from 2000 to 2020. *Remote Sensing* **13**: 1332.

Noss RF, Laroe ET III, Scott JM. 1995. *Endangered ecosystems of the United States: a preliminary assessment of loss and degradation*. Biological Report 28. Washington, DC, USA: U.S. National Biological Service.

O'sullivan O, Heskel MA, Reich PB, Tjoelker MG, Weerasinghe LK, Penillard A, Zhu L, Egerton JJ, Bloomfield KJ, Creek D *et al.* 2017. Thermal limits of leaf metabolism across biomes. *Global Change Biology* **23**: 209–223.

O'Sullivan OS, Weerasinghe KWLK, Evans JR, Egerton JJG, Tjoelker MG, Atkin OK. 2013. High-resolution temperature response of leaf respiration in snow gum (*Eucalyptus pauciflora*) reveal high-temperature limits to respiratory function. *Plant, Cell & Environment* **36**: 1268–1284.

Overpeck JT, Udall B. 2020. Climate change and the aridification of North America. *Proceedings of the National Academy of Sciences, USA* **117**: 11856–11858.

Perez T, Feeley KJ. 2020. Photosynthetic heat tolerances and extreme leaf temperatures. *Functional Ecology* **34**: 2236–2245.

Pezeschki SR, Hinckley TM. 1988. Water relations characteristics of *Alnus rubra* and *Populus trichocarpa*: responses to field drought. *Canadian Journal of Forest Research* **18**: 1159–1166.

Poorter H, Remkes C. 1990. Leaf area ratio and net assimilation rate of 24 wild species differing in relative growth rate. *Oecologia* **83**: 553–559.

Posch BC, Hammer J, Atkin OK, Bramley H, Ruan Y-L, Trethowan R, Coast O. 2022. Wheat photosystem II heat tolerance responds dynamically to short- and long-term warming. *Journal of Experimental Botany* **73**: 3268–3282.

PRISM Climate Group. 2022. PRISM Climate Group, OR State University. [WWW document] URL https://prism.oregonstate.edu [accessed 24 May 2022].

R Core Team. 2019. *R: a language and environment for statistical computing*. Vienna, Austria: R Foundation for Statistical Computing.

Rood SB, Braatne JH, Hughes FMR. 2003. Ecophysiology of riparian cottonwoods: streamflow dependency, water relations and restoration. *Tree Physiology* **23**: 113–1124.

Russo S, Sillmann J, Sippel S, Barcikowska MJ, Ghesetti SM, O'Neill B. 2019. Half a degree and rapid socioeconomic development matter for heatwave risk. *Nature Communications* **10**: 136.

Schreiber U, Barry J. 1977. Heat-induced changes in chlorophyll fluorescence in intact leaves correlated with damage to the photosynthetic apparatus. *Planta* **136**: 233–238.

Schulte PJ, Hinckley TM. 1985. A comparison of pressure volume curve data analysis and techniques. *Journal of Experimental Botany* **36**: 1590–1602.

Schweitzer JA, Martinsen GD, Whitham TG. 2002. Cottonwood hybrids gain fitness traits of both parents: a mechanism for their long-term persistence? *American Journal of Botany* **89**: 981–990.

Seemann JR, Downton WJS, Berry JA. 1986. Temperature and leaf osmotic potential as factors in the acclimation of photosynthesis to high temperature in desert plants. *Plant Physiology* **80**: 926–930.

Slot M, Cala D, Aranda J, Virgo A, Michaletz ST, Winter K. 2021. Leaf heat tolerance of 147 tropical forest trees species varies with elevation and leaf functional traits, but not with phylogeny. *Plant, Cell & Environment* **44**: 2414–2427.

Snyder KA, Williams DG. 2000. Water sources used by riparian trees varying among stream types on the San Pedro River. *Agricultural and Forest Meteorology* **105**: 227–240.

Still CJ, Page G, Rastogi B, Griffith DM, Aubrecht DM, Kim Y, Burns SP, Hanson CV, Kwon H, Hawkins L *et al.* 2022. No evidence of canopy scale leaf thermoregulation to cool leaves below air temperature across a range of forest ecosystems. *Proceedings of the National Academy of Sciences, USA* **119**: e2205682119.

Stromberg JC. 1993. Frémont cottonwood-Goodding willow riparian forests: a review of their ecology, threats and recovery potential. *Journal of the Arizona-Nevada Academy of Sciences* **27**: 97–110.

Tapiador FJ, Navarro A, Moreno R, Luis SJ. 2020. Regional climate models: 30 years of dynamical downscaling. *Atmospheric Research* **235**: 104785.

Tillman FD, Gangopadhyay S, Pruit T. 2020. *Trends in recent historical and projected climate data for the Colorado River Basin and potential effects on groundwater availability: US Geological Survey Scientific Investigations Report 2020–5107*. 24 p. doi: 10.3133/sir20205107.

Tyree MT, Ewers FW. 1991. Tansley review no. 34: the hydraulic architecture of trees and other woody plants. *New Phytology* **119**: 345–360.

Watanabe M, Suzuki T, O'ishi R, Komuro Y, Watanabe S, Emori S, Takemura T, Chikira M, Ogura T, Sekiguchi M *et al.* 2010. Improved climate simulation by MIROC5: mean states, variability, and climate sensitivity. *Journal of Climate* **23**: 6312–6335.

Weis B, Berry JA. 1988. Plants and high temperature stress. *Symposia of the Society of Experimental Biology* **42**: 329–346.

Whitham TG, Gehring CA, Bothwell HM, Cooper HF, Hull JB, Allan GJ, Grady KC, Markovchick L, Shuster SM, Parker J *et al.* 2020. Using the Southwest experimental garden array to enhance riparian restoration in response to global environmental change: identifying and deploying genotypes and populations for current and future environments (Chapter 4). In: Carothers SW, Johnson RR, Finch DM, Kingsley KJ, Hamre RH, eds. *Riparian research and management past, present and future, vol. 2*. General Technical Report RMRS-GTR-411. Washington, DC, USA: Department of Agriculture, Forest Service, Rocky Mountain Research Station, 63–79.

Williams AP, Cook BI, Smerdon JE. 2022. Rapid intensification of the emerging southwestern North American megadrought in 2020–2021. *Nature Climate Change* **12**: 232–234.

Williams AP, Cook ER, Smerdon JE, Cook BI, Abatzoglou T, Bolles K, Baek SH, Badger AM, Livneh B. 2020. Large contribution from anthropogenic warming to an emerging North American megadrought. *Science* **368**: 314–318.

Wobus C, Zarakas C, Malek P, Sanderson B, Crimmins A, Kolian M, Sarofim M, Weaver CP. 2018. Reframing future risks of extreme heat in the United States. *Earth's Future* **6**: 1323–1335.

Woodhouse CA, Meko DM, Macdonald GM, Stahle DW, Cook ER. 2010. A 1200-year perspective of 21st century drought in southwestern North America. *Proceedings of the National Academy of Sciences, USA* **107**: 21283–21288.

Yi K, Smith JW, Jablonski AD, Tatham EA, Scanlon TM, Lerdau MT, Novick KA, Yang X. 2020. High heterogeneity in canopy temperature among co-occurring tree species in a temperate forest. *Journal of Geophysical Research: Biogeosciences* **125**: e2020JG005892.

Zhao L, Oleson K, Bou-Zeid E, Krayenhoff ES, Bray A, Zhu Q, Zheng Z, Chen C, Oppenheimer M. 2021. Global multi-model projections of local urban climates. *Nature Climate Change* **11**: 152–157.

Zscheischler J, Seneviratne SI. 2017. Dependence of driver affects risks associated with compound events. *Science Advances* **3**: e1700263.

Supporting Information

Additional Supporting Information may be found online in the Supporting Information section at the end of the article.

Dataset S1 Watershed of source population, elevation of source population, transfer distance of source population, genotype

code, and measured traits of *Populus fremontii* genotypes at a common garden near Yuma, AZ, USA, in May 2021.

Dataset S2 Watershed of source population, elevation of source population, transfer distance of source population, genotype code, and measured traits of *Populus fremontii* genotypes at a common garden near Yuma, AZ, USA, in May 2021.

Dataset S3 Watershed of source population, elevation of source population, transfer distance of source population, genotype code, and measured traits of *Populus fremontii* leaves collected from mature trees in July 2022 at source site locations.

Fig. S1 Diameter at root crown and tree height in relation to transfer distance measured in May 2021, on *Populus fremontii* genotypes at an experimental common garden near Yuma, AZ, USA.

Fig. S2 Example of the temperature-F_o response curve yielded from the Closed Photon Systems Instruments, FC-800-C FluorCam fluorescence imager coupled to a TR2000 thermoregulator ($n = 45$ *Populus fremontii* leaves).

Fig. S3 Weather conditions at the experimental common garden near Yuma, AZ, USA, from 3 May 2021 to 21 August 2021, including maximum, minimum and mean daily temperatures, and maximum, minimum and mean daily vapor pressure deficit.

Fig. S4 Comparison of T_{crit} values measured on sunlit *Populus fremontii* leaves in July 2022 at source population locations with T_{crit} values reported in 177 species from O'Sullivan *et al.* (29) spanning a 25 plus °C range in mean maximum temperatures of the warmest month.

Fig. S5 Relationship between maximum leaf temperature subtracted from air temperature (ΔT_{leaf}) and minimum daytime stomatal conductance (g_{smin}) of *Populus fremontii* genotypes at an experimental common garden near Yuma, AZ, USA.

Fig. S6 Predawn (Ψ_{pd}) and minimum daytime (Ψ_{min}) leaf water potentials in relation to transfer distance in *Populus fremontii* genotypes at an experimental common garden near Yuma, AZ, USA.

Table S1 Description of site locations including site elevation, and transfer distance from the common garden in Yuma, AZ, USA.

Please note: Wiley is not responsible for the content or functionality of any Supporting Information supplied by the authors. Any queries (other than missing material) should be directed to the *New Phytologist* Central Office.